UNEC Journal of Engineering and Applied Sciences
Vol. 5, No.2, 2025, pp. 127-133
DOI: https://doi.org/10.61640/ujeas.2025.1212

SECTION:
CHEMISTRY &
MATERIALS SCIENCE

The character of interaction in the Dy-As-Se system

T.M. Ilyasly[1], R.F. Abbasova[1*], S.M. Veysova[1], G.H. Gahramanova[1], A.Y. Suleymanova[2], M.A. Huseynov[2]

[1]Department of General and Inorganic Chemistry, Faculty of Chemistry, Baku State University, 23 Z. Khalilov str., Baku AZ1148, Azerbaijan
[2]Department of Engineering and Applied Sciences, Azerbaijan State University of Economics (UNEC), 6 Istiglaliyyat str, Baku AZ1001, Azerbaijan
email: *ranaabbasova@bsu.edu.az*

Abstract

The nature of chemical interaction in the Dy-As-Se ternary system was examined across As_2Se_3-Dy, As_2Se_3-DySe, As_2Se_3-Dy_2Se_3 sections using comprehensive set of physicochemical analysis techniques. These included differential thermal analysis (DTA), X-ray powder diffraction (XRD), microstructural analysis (MSA), microhardness measurement and density determination. The boundaries of glass-forming regions in the systems were determined at different cooling rates: specifically quenching in air and in ice water.

The observed increase in macroscopic properties suggest the formation of of new structural units in glassy state, in additional to the trigonal $AsSe_{2/3}$ structural unit As_2Se_3 characteristic of the glass network. Formation of new structural units within the glassy phase. In the studied sections based on the glass-forming compound, a region of homogeneity was identified. Furthermore, an optimal synthesis regime for preparation of dysprosium-containing chalcogenide glasses was determined.

***Keywords*:** phase diagram, ternary system, glasses, semiconductors.
PACS numbers: 64.70.P, 74.81.Bd, 81.30.Bx

Received:	*Revised:*	*Accepted:*	*Published:*
29 June 2025	*17 August 2025*	*10 December 2025*	*30 December 2025*

1. Introduction

Chalcogenide based materials are widely investigated due to various attractive properties applicable in broad range of areas. Depending on the elemental composition and synthesis condition, these types of materials obtained in different structural forms, such as layered, glassy etc. [1-9] Among them, chalcogenide glassy substances derived from glass-forming compounds, particularly arsenic sulfides and selenides, are promising materials for electronic and optoelectronic applications.

The development of novel synthesis strategies for multifunctional materials remains a key challenge in contemporary inorganic chemistry [10-15].

Binary and ternary rare-earth elements (REE) chalcogenides exhibit a range of distinctive physicochemical properties, enabling their use in advance technological fields, including semiconductor devices, ferro- and antiferromagnetic systems [16-23].

In addition, these materials are employed in the fabrication of specialized glasses for nuclear engineering, such as luminescent materials [24-26].

Chalcogenide glasses exhibit low optical losses over a broad spectral range from 0.5 to 0.20 μm with the exact transmission window depending on the glass composition. Optical

fibers fabricated from REE doped chalcogenide glasses, where REEs belong to group 3 in the periodic table, are widely used in the development of infrared (IR) lasers, optical amplifiers, and broadband radiation sources. Despite expensive investigations of REE luminescence in various chalcogenide glass matrices in the mid-IR region, the influence of activator ions on the optical properties of doped chalcogenide glasses near the fundamental absorption band edge remains insufficient understood. For chalcogenide glasses, this spectral region corresponds to wavelengths of approximately 0.8-2 μmin the near IR range.

Notably, this region also encompasses the absorption band of REE ions commonly employed for luminescence excitation using available laser sources. Previous studied have shown that, in dysprosium-doped glasses, the optical response in the weak-absorption region is governed not only by glass matrix but also by electric transitions between energy levels of Dy^{3+} ions. Moreover, energy transfer between rare-earth ions and localized states within the glass band gap may result in luminescence quenching, which must be considered in the design of laser devices based on these materials [13-15].

Nevertheless, the practical development of chalcogenide glasses remains challenging, as their infrared efficiency often does not meet the requirement for device applications. Therefore, the aim of this study is to develop an optimized synthesis approach for arsenic selenide-based chalcogenide glasses doped with dysprosium ions.

Incorporation of REEs into chalcogenide glass matrices enhances the ionic character of chemical bonding, which in turn reduces the glass forming region.

In this study, systems containing arsenic and dysprosium selenides were investigated to advance fundamental understanding of structure-properties relationships in chalcogenide materials.

2. Experimental

Chemicals and materials

The Dy-As-Se system was studied along various sections. The alloys were synthesized from high- purity elemntal components: dysprosium (Dy, grade A1); arsenic (As, grade B5); and selenium (Se, grade B4).

Synthesis of the alloy system was performed in rotary furnaces using a stepwise heating protocol. The samples were initially held at 750K for 10-12 hours, after which the temperature was increased to 1050 K and maintained for 2 hours to ensure homogenization. Subsequently, the furnace was cooled at a controlled rate of 10 $K \cdot min^{-1}$.

Characterization methods

The synthesized alloys were characterized using a combination of physicochemical analysis techniques. Differential thermal analysis (DTA) was conducted using Kurnakov pyrometer and a Termoskan-2 instrument. DTA measurements were performed up to 1000 K using a chromel-alumel thermocouple.

X-ray powder diffraction (XRD) pattern were recorded on a diffractometer, on a D-2 PHASER diffractometer employing CuK_α radiation with a Ni filter

For microstructural analysis (MSA), the samples were etchant using a mixture of concentrated HNO_3 and H_2O_2 in a 1:1 volume ratio with an etching duration of 15-20 s. The etched surfaces of samples were examined by optical microscopy using a MIN-8 and MIM-7 microscope on polished sections prepared with GOI paste.

The microhardness of the glassy alloys was measured using a PMT-3 microhardness tester under applied loads of 15 and 20 g, depending on composition. The measurement uncertainty ranged from 2.2 to 4.3%.

The density of the alloys was determined by the pycnometer, with toluene used as the immersion liquid.

3. Results and discussion

The alloys of the Dy-As-Se system synthesized along As_2Se_3-Dy, As_2Se_3-DySe, As_2Se_3-Dy_2Se_3 sections were systematically investigated.

The As_2Se_3-Dy system. The compositions of alloys studied in the As_2Se_3-Dy section and some of their physicochemical properties are summarized in table 1.

Composition, at. %		Thermal effects			Microhardness H_μ, MPa	Density, g/cm^3	Results of microstructural analysis
As_2Se_3	Dy	T_g	T_{cr}	T_m			
100	0	180	-	380	1228	4,50	Single-turbid phase
97	3	190	258	385	1350	4,60	Single-turbid phase
95	5	195	265	369	1360	4,80	Single-turbid phase
93	7	195	270	375	1365	4,85	Single-turbid phase
90	10	205	280	365	1370	4,90	Single-turbid phase

Table 1. Compositions and some physicochemical properties of alloys of the As_2Se_3-Dy system (cooling rate 10 K/min)

The synthesized glassy alloys are soluble in concentrated nitric acid and in alkaline solutions (NaOH and KOH), but are insoluble in organic solvents and water.

Microscopic examination revealed no crystalline inclusions. Consistent with these observations, X-ray phase analysis show no distinct diffraction peaks inherent to crystalline substances. Differential thermal analysis thermograms of alloys containing up to 7 at.% Dy are shown in figure 1.

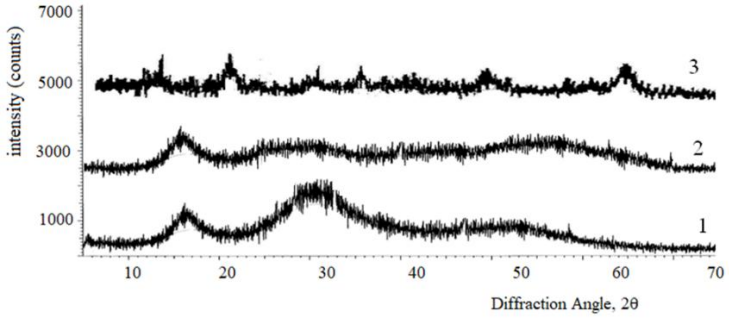

Figure 1. XRD results of alloys of the system As_2Se_3-Dyb 1- As_2Se_3, 2-3 at.% Dy, 3-7 at.% Dy

Three thermal effects were found on the thermograms of alloys of the As_2Se_3-Dy system.

Tg - glass formation temperature, Tcr- crystallization temperature, Tm- melting temperature.

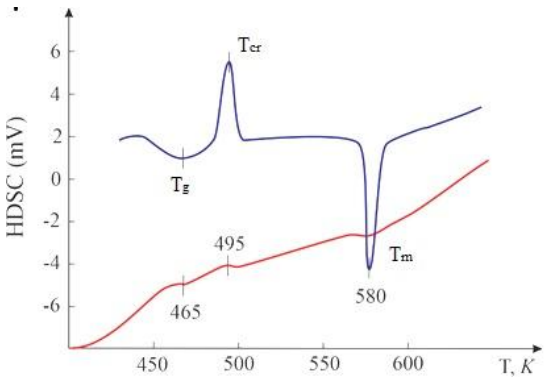

Figure 2. Thermogram of the alloy containing 7 at.% Dy

Based on the DTA results, a microstructural diagram of the As_2Se_3-Dy system was constructed, figure 3.

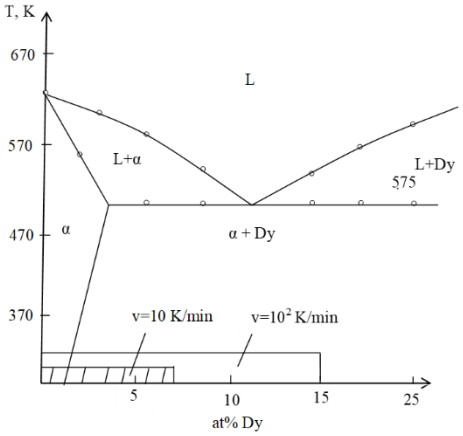

Figure 3. Microstructural diagram of the As_2Se_3-Dy system

As follow from the diagram, the homogeneity region based on As_2Se_3 expends up to 1,5 at.% Dy at room temperature. Microstructural analysis was performed using an etchant composed of NaOH and C_2H_5OH in a 1:1 volume ratio.

The synthesis of alloys in this system was conducted following the same procedure as that used for the As_2Se -Dy system. After synthesis, the alloys were cooled at a rate of 10 и 10^2 K/min. Two areas of glass formation were identified along this section. It was established that the glass -forming regions of in this system upon cooling at a rate of 10 K/min and 10^2 K/min extend to 7 and 15 at. % Dy, respectively.

The As_2Se_3-DySe system. Based on the data obtained by combination of physicochemical analysis techniques, a Microstructural diagram of the As_2Se_3-DySe system (figure 4) was constructed following crystallization of the alloys.

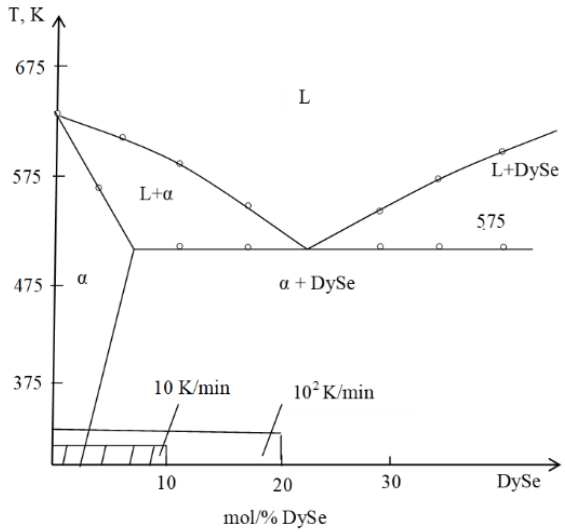

Figure 4. Microstructural diagram of the As_2Se_3-DySe system

The homogeneity region based on As_2Se_3 extends to 2 mol.% DySe at room temperature. It was established that upon cooling at a rate of 10 K/min and 10^2 K/min the glass-forming region in the system expands to 10 and 20 mol. % DyS**e**, respectively. Complete crystallization of glassy alloys was confirmed by microstructural analysis and X-ray diffraction. As evident from the phase diagram, an increase in DySe content leads to a corresponding enhancement of macroscopic properties (table 2).

№	Composition, mol.%		Thermal effects			Microhardness MPa	Density, g/cm^3
	As_2Se_3	DySe	T_g	T_{cr}	T_m		
1	100	0	180	-	380	1300	4,52
2	99	1	185	250	380	1340	4,54
3	97	3	180	220	375	1350	4,58
4	95	5	185	225	375	1350	4,60
5	90	10	190	230	370	1380	4,65
6	80	20	200	240	360	1410	4,80

Table 2. Compositions and some physicochemical properties of alloys of the As_2Se_3-Dy_2Se_3 system (cooling rate 10 K/min)

The As_2Se_3-Dy_2Se_3 system. Investigation of the alloys in this system revealed the formation of glassy phase. The extent of the glass-forming region was found to depend strongly on the cooling rate: at 10 K/min the glass-forming region is relatively narrow, whereas increasing the cooling rates to 10^2 K/min leads to significant expansion of this region. Specifically, the glass-forming region extends to 12 and 25 mol. % Dy_2Se_3 at cooling at a rate of 10 K/min and 10^2 K/min, respectively.

Following crystallization of the alloys, a microphase diagram of the As_2Se_3-Dy_2Se_3 system was constructed (figure 5).

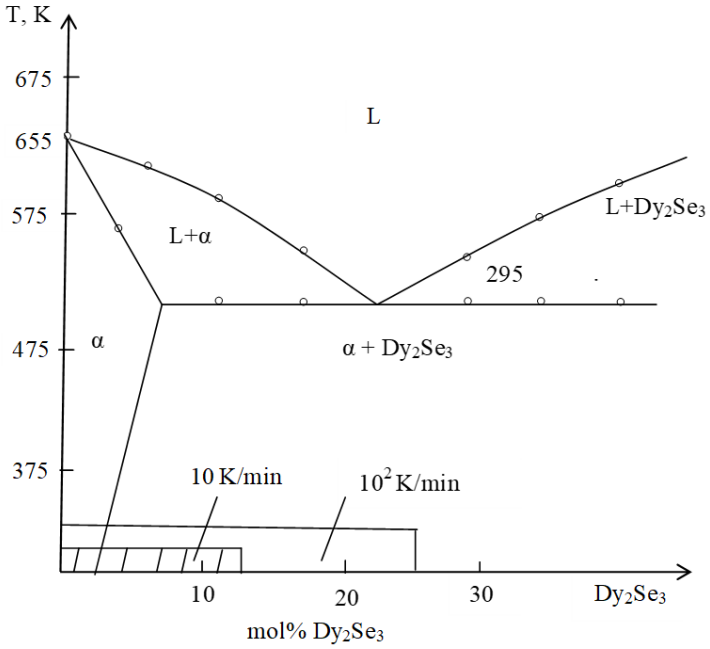

Figure 5. Microstructural diagram of the As_2Se_3-Dy_2Se_3 system

№	Composition, mol.%		Thermal effects of heating			Microhardness MPa	Density, g/cm^3
	As_2Se_3	Dy_2Se_3	T_g	T_{cr}	T_m		
1	100	0	450	-	650	1300	4,58
2	99	1	455	520	640	1350	4,65
3	97	3	466	525	635	1380	4,68
4	95	5	474	530	630	1420	4,75
5	93	7	480	545	635	1450	4,81
6	90	10	485	555	640	1475	5,10
7	85	15	490	560	650	1495	5,15

Table 3. Compositions and some physicochemical properties of alloys of the As_2Se_3-Dy_2Se_3 system (cooling rate 10 K/min)

The homogeneity region based on As_2Se_3 reaches to 2.3 mol.% Dy_2Se_3 at room temperature. Table 3 shows the results of the physicochemical analysis of the alloys of the As_2Se_3-Dy_2Se_3 system.

The introduction of up to 15 mol.% Dy_2Se_3 into the As_2Se_3 composition results in the formation of glassy alloys.

The chemical interaction can be represented by the preferential reactions of selenium with dysprosium, followed by its interaction with arsenic. This conclusion is supported by estimates of the binding energy and by the relative magnitude of the standard Gibbs free energies.

Analysis of the macroscopic properties, including the glass transition temperature (Tg), density (d), and microhardness (Hμ) indicates that in addition to trigonal $As_2Se_{3/2}$ structural units, new tetragonal structural units are formed in the resulting glassy samples

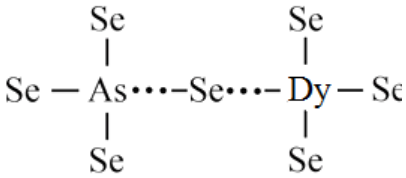

4. Conclusion

The results of our studies demonstrate that the glass-forming region is governed by the extent of the arsenic triselenide phase, indicating that the intrinsic nature of the constituent substance plays a critical role in glass formation.

An optimal synthesis regime was established for As_2Se_3 based glasses incorporating the rare earth element dysprosium Dy in the form of Dy, DySe, Dy_2Se_3.

Analysis of the experimental data, including observed increase in macroscopic properties, suggests the formation of additional new structural units involving Dy, alongside the trigonal $As_2Se_{3/2}$ structural units.

In the studied sections based on the glass-forming compound, a region of homogeneity was identified, which expands in the sequence Dy → DySe → Dy_2Se_3.

On the basis of differential thermal analysis, X-ray diffraction results, microstructural diagrams of the As_2Se_3-Dy, As_2Se_3-DySe, As_2Se_3-Dy_2Se_3 systems were constructed.

Authors'Declaration

Conflicts of Interest: We have no conflicts of interest to disclose

Authors' Contribution Statement

Ilyasly T.M provided resources, wrote the first draft of the manuscript, and supervised the project.

Abbasova R.F. analyzed the data and contributed to the interpretation of the results

Gahramanova G.H. conducted the experiments

Veysova S.M. conducted the experiments

All authors reviewed and approved the final manuscript.

References

1. A.Sh. Abdinov, R.F. Babayeva, S.I. Amirova, N.A. Rahimova, E.A. Rasulov, UNEC J. Eng. Appl. Sci. **5**(1) (2025) 55.
2. A.I. Isayev, S.I. Mekhtiyeva, H.I. Mammadova, R.I. Alekberov, Q.M. Ahmadov, N.N. Eminova, A.Ch. Mammadova, L.A. Aliyeva, L.V. Afandiyeva, R.F. Sadikhli, UNEC J. Eng. Appl. Sci. **4**(1) (2024) 55.

3. I.I. Aliyev, Kh.M. Gashimov, C.A. Ahmedova, UNEC J. Eng. Appl. Sci. **2**(1) (2022) 45.
4. T.G. Naghiyev, U.R. Rzayev, E.M. Huseynov, I.T. Huseynov, S.H. Jabarov, UNEC J. Eng. Appl. Sci. **2**(1) (2022) 85.
5. T.G. Naghiyev, R.F. Babayeva, A.S. Abiyev, Eur. Phys. J. B **97** (2024) 131.
6. A.S. Abdinov, R.F. Babaeva, Inorg. Mater. **57** (2021) 119.
7. T.D. Ibragimov, A.M. Hashimov, G.B. Ibragimov, R.M. Rzayev, Fullerenes, Nanotubes and Carbon Nanostructures **29(**12) (2021) 951.
8. F. Behmagham, S. Arshadi, E. Vessally, T.G. Naghiyev, R. Rzayev, D. Sur, S. Ganesan, Computational and Theoretical Chemistry **1243** (2025) 114976.
9. R. Behjatmanesh-Ardakani, R. Rzayev, Chemical Review and Letters, **7**(6) (2024) 1022.
10. T. Ilyasli, D. Hasanova, Z. Ismaylov, Photosensitive material, Azerbaijan Patent No. **I 2022 0047**, Azerbaijan BSU (2022).
11. T. Ilyasli, Q. Qahramanova, Z. Ismaylov, Chalcogenide glass, Azerbaijan Patent No. **I 2021 0046**, Azerbaijan BSU (2021).
12. B. Karasu, T. İdinak, E. Erkol, A.O. Yanar, El-Cezerî Journal of Science and Engineering **6**(3) (2019) 428.
13. Yu.S. Kuzyutkina, N.D. Parshina, E.A. Romanova, V.I. Kochubey, M.V. Sukhanov, L.A. Ketkova, V.S. Shiryaev, Optics and Spectroscopy **131**(1) (2023) 14.
14. H. Guo, J. Cui, C. Xu, Y. Xu, G. Farrell, in: Mid-Infrared Fluoride and Chalcogenide Glasses and Fibers, Springer: Singapore (2022) pp.217, 283.
15. M.V. Sukhanov, A.P. Velmuzhov, M.F. Churbanov, B.I. Galagan, B.I. Denker, V.V. Koltashev, V.G. Plotnichenko, S.E. Sverchkov, Photon-Express-Science **6** (2021) 86.
16. G.H. Gakhramanova, Baku University News. Natural Sciences Series **2** (2021) 27.
17. V.G. Nenajdenko, A.A. Kazakova, A.S. Novikov, N.G. Shikhaliyev, A.M. Maharramov, A.M. Qajar, G.T. Atakishiyeva, A.A. Niyazova, V.N. Khrustalev, A.V. Shastin, Catalysts **13**(8) (2023) 1194.
18. T.M. Ilyasly, A.G. Khudieva, Z.I. Ismailov, R.F. Abbasova, L.A. Mamedova, I.I. Aliyev, in: Proceedings of the International Scientific and Practical Conference, Belgorod (2017) 44.
19. Z. Atioglu, M. Akkurt, N.Q. Shikhaliyev, U.F. Askerova, A.A. Niyazova, S. Mlowe, Acta Crystallographica Section E **77**(8) (2021) 829.
20. T. Ilyasly, R. Abbasova, S. Veysova, G. Gahramanova, New Materials, Compounds and Applications **7**(3) (2023) 210.
21. M. Akkurt, A.M. Maharramov, N.G. Shikhaliyev, A.M. Qajar, G.T. Atakishiyeva, I.M. Shikhaliyeva, A.A. Niyazova, A. Bhattarai, UNEC Journal of Engineering and Applied Sciences **3**(1) (2023) 33.
22. R.M. Mawale, M.V. Ausekar, L. Prokeš, V. Nazabal, E. Baudet, T. Halenkovič, M. Bouška, M. Alberti, P. Němec, J. Havel, Journal of the American Society for Mass Spectrometry **28** (2017) 2569.
23. M. Kudryashov, L. Mochalov, A. Nezdanov, R. Kornev, A. Logunov, D. Usanov, A. Mashin, G. De Filpo, D. Gogova, Superlattices and Microstructures **128** (2019) 334.
24. P.K. Singh, D.K. Dwivedi, Ferroelectrics **520**(1) (2017) 256.
25. N. Syrbu, V. Zalamai, Optoelectronics and Advanced Materials – Rapid Communications **13**(9–10) (2019) 530.
26. Y. Wang, G. Zhu, S. Xin, Q. Wang, Y. Li, Q. Wu, C. Wang, X. Wang, X. Ding, W. Geng, Journal of Rare Earths **33**(1) (2015) 1.